Supporting Information

A Biomimetic Nanofluidic Tongue for Highly Selective and Sensitive Bitter Perception

Yanan Li,[a] Hua Zheng,[a] Lei Xu,[a] Linfeng Chen,*[,a] Fan Xia,[a] and Yanlin Song [b]

[a]State Key Laboratory of Geomicrobiology and Environmental Changes, Engineering Research Center of Nano-Geomaterials of Ministry of Education, Faculty of Materials Science and Chemistry, China University of Geosciences, Wuhan 430074, China; Email: chenlinfeng@cug.edu.cn

[b]Key Laboratory of Green Printing, CAS Research/Education Center for Excellence in Molecular Sciences, Institute of Chemistry, Chinese Academy of Sciences (CAS), Beijing 100190, P. R. China

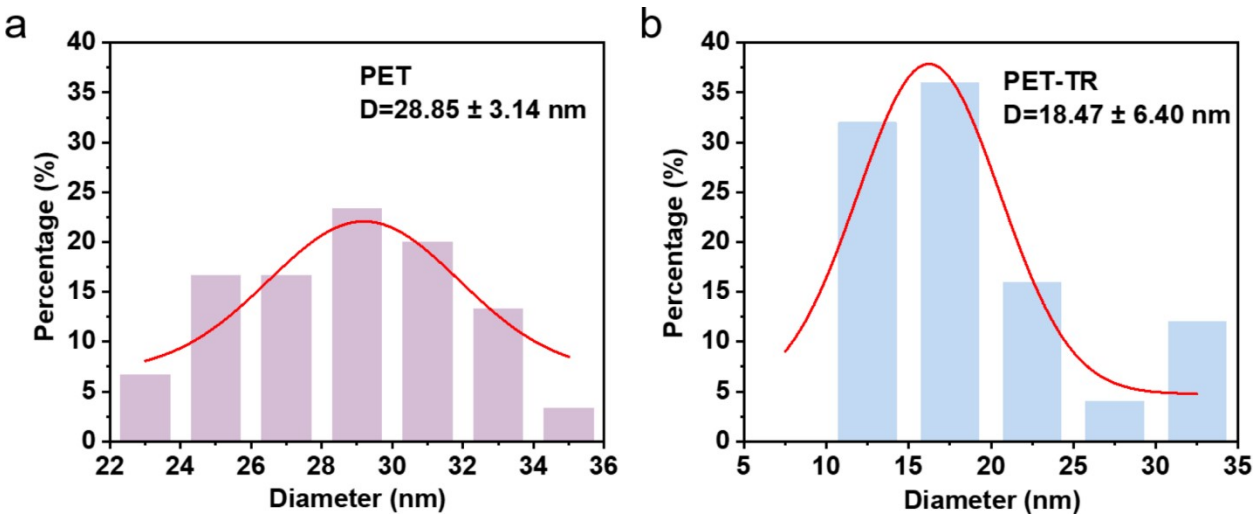

Figure S1. Diameter distribution of (a) PET and (b) PET-TR nanochannels membranes.

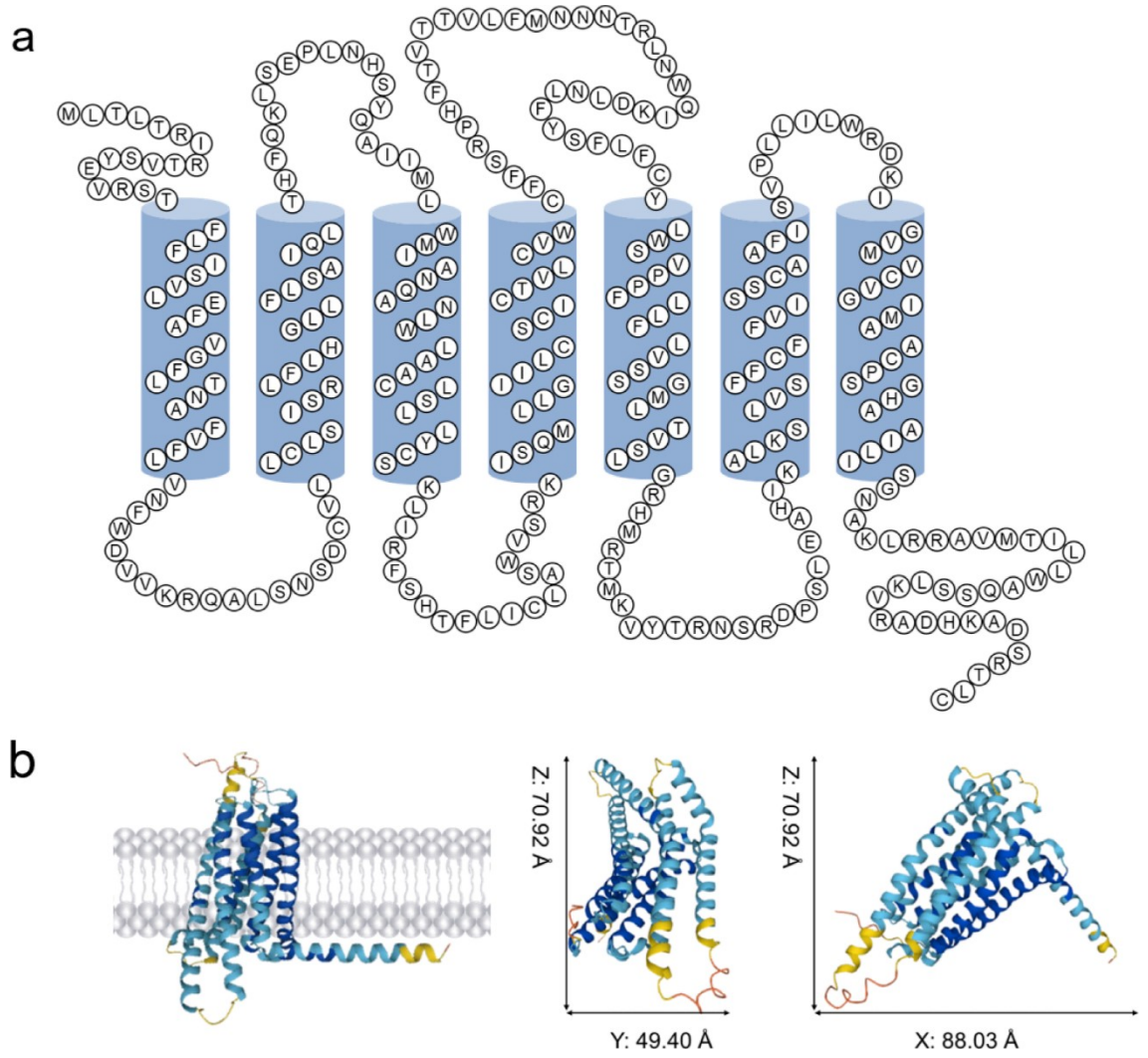

Figure S2. Bitter receptor T2R38. (a) The sequence status, Structure (UniProt: P59533) and (b) The diameter size of T2R38.

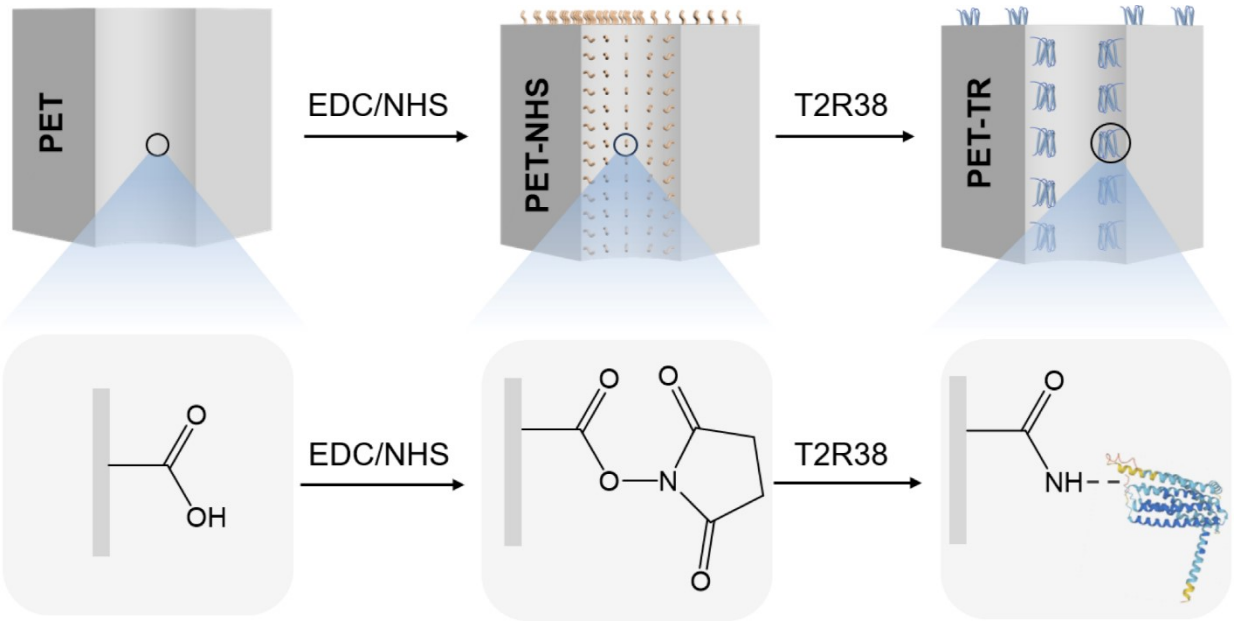

Figure S3. Schematic diagram of the construction process of PET bitter sensor.

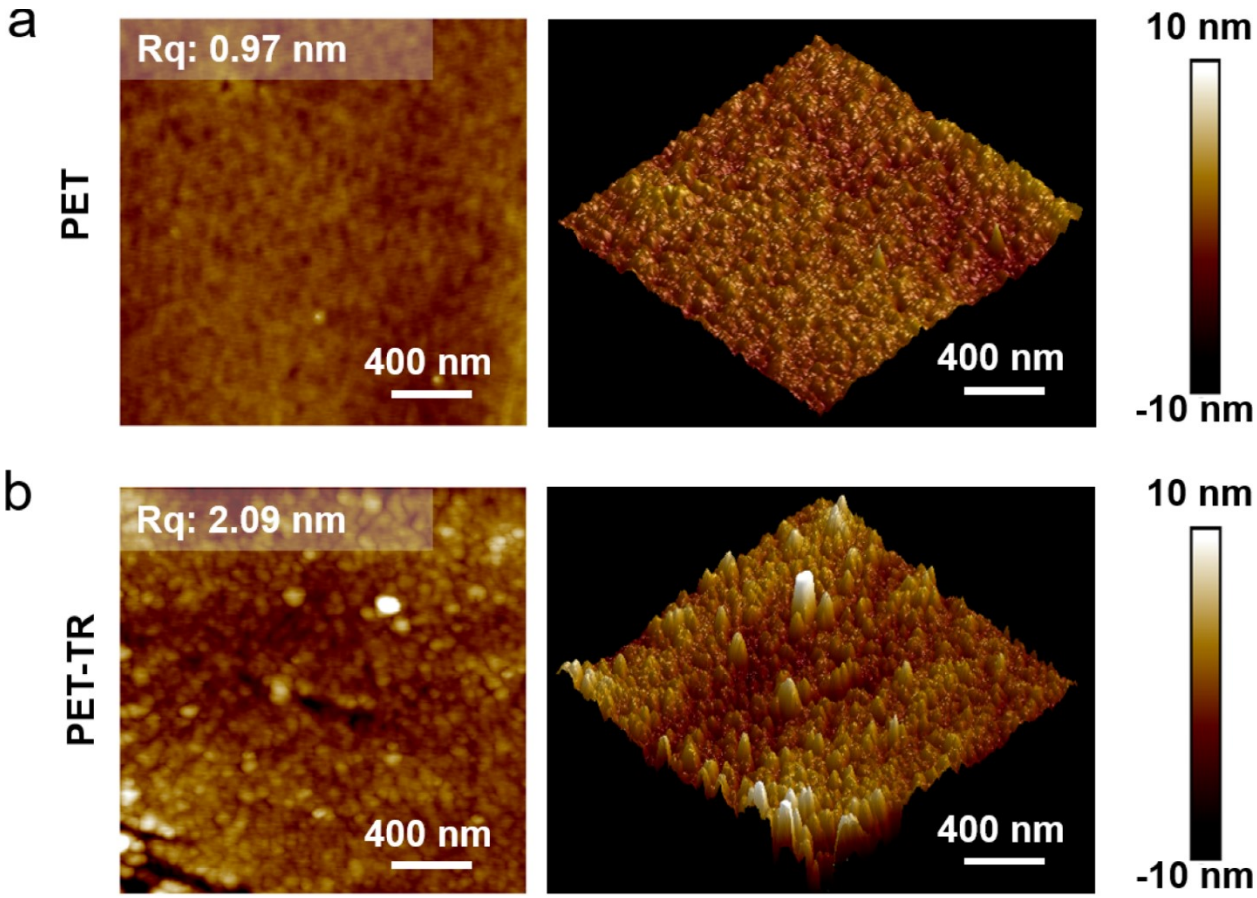

Figure S4. Two-dimensional and corresponding three-dimensional atomic force microscopy images of (a) PET and (b) PET-TR nanochannels membranes. The surface roughness (Rq) increased from 0.97 nm to 2.09 nm after protein modification.

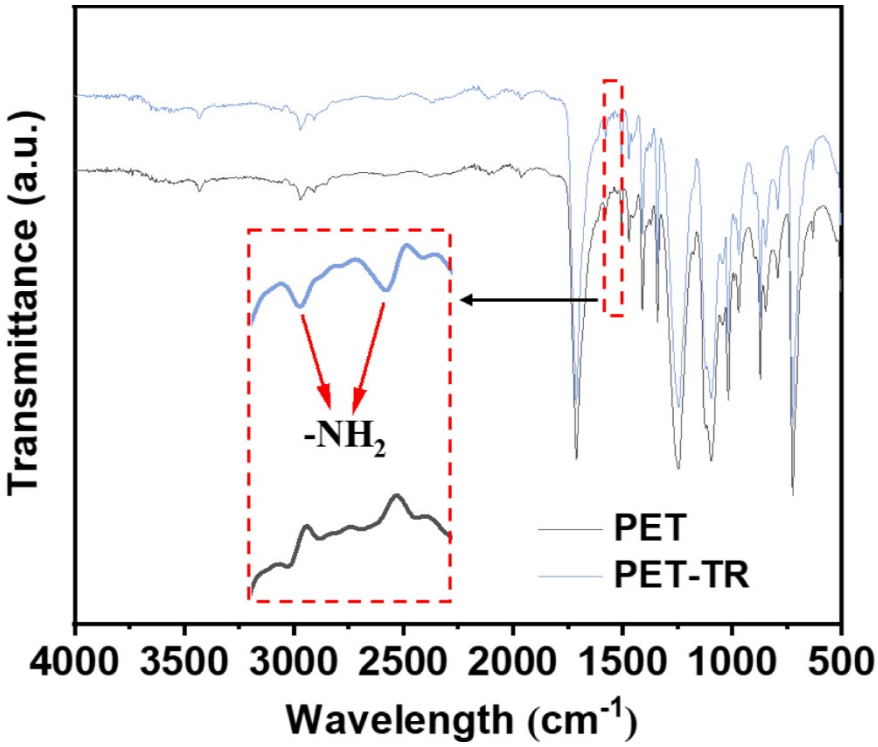

Figure S5. FTIR spectra of PET and PET-TR membranes.

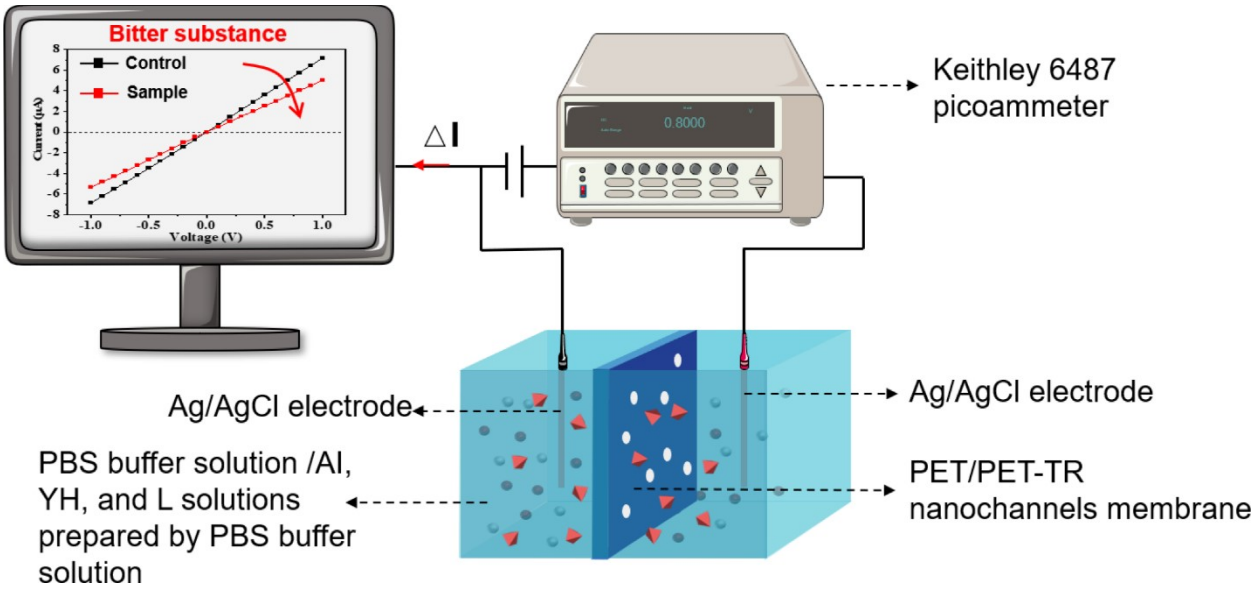

Figure S6. Experimental device diagram of biomimetic bitter sensor for detecting bitter substances.

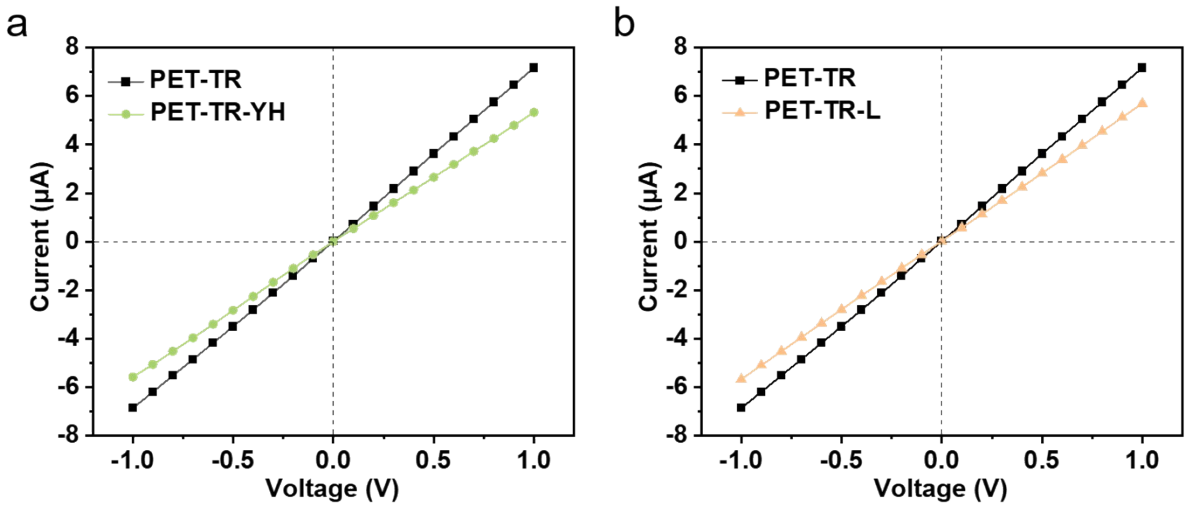

Figure S7. *I-V* curves after the (a) YH and (b) L (10^{-4} M) are captured by the bioinspired nanochannel-based platform for bitter detection.

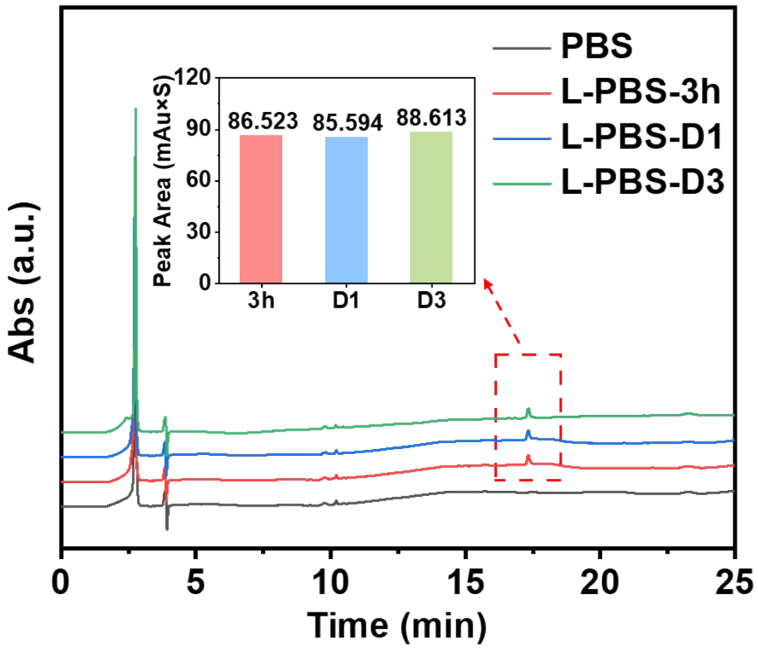

Figure S8. Stability assessment of 10^{-4} M limonin prepared in PBS buffer solution (pH 7.4) via HPLC analysis. The characteristic peak of limonin was consistently observed at 17.32 min. The peak areas for the samples L-PBS-3h (after 3 hours), L-PBS-D1 (after 1day), and L-PBS-D3 (after 3 days) were 86.523 mAu×s, 85.594 mAu×s, and 88.613 mAu×s, respectively. The minimal variation in these values indicate that limonin remains relatively stable in the PBS buffer (pH 7.4) over the three-day test period.

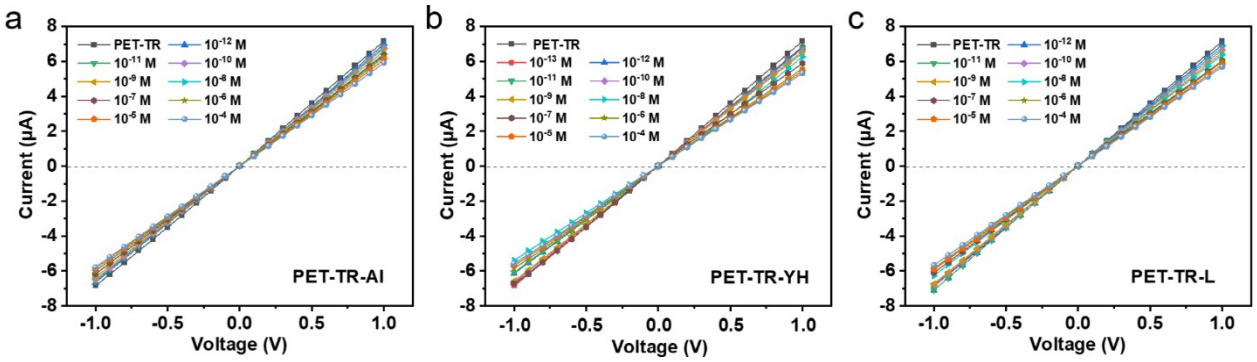

Figure S9. *I-V* curves of PET-TR membranes in response to different concentrations of (a) AI, (b) YH and (c) L.

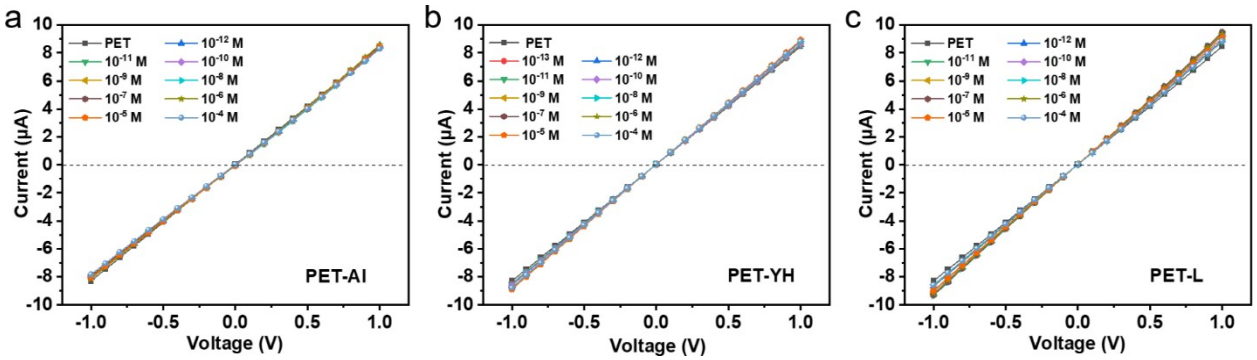

Figure S10. *I-V* curves of PET membranes without T2R38 modification in response to different concentrations (a) AI, (b) YH and (c) L.

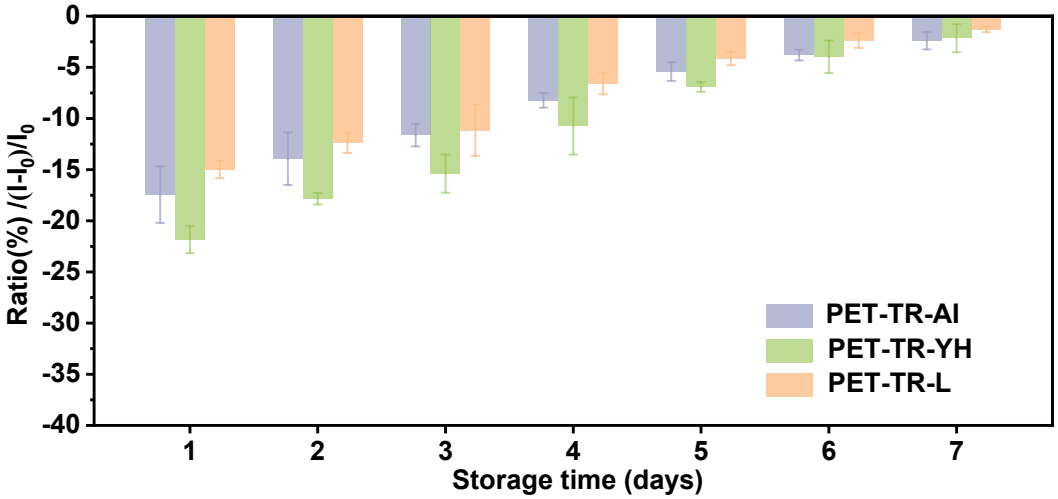

Figure S11. Stability evaluation of PET-TR stored at room temperature over a 7-day storage period under experimental conditions. The results indicate that the activity of the bitter sensor gradually decreased when stored at room temperature for 7 days. It retained 66.67%, 70.50%, and 74.459% for AI, YH, and L in 3 days, respectively. However, after 7 days, the sensor retained only 13.79%, 9.86%, and 8.74% of its original detection performance for AI, YH, and L, respectively.

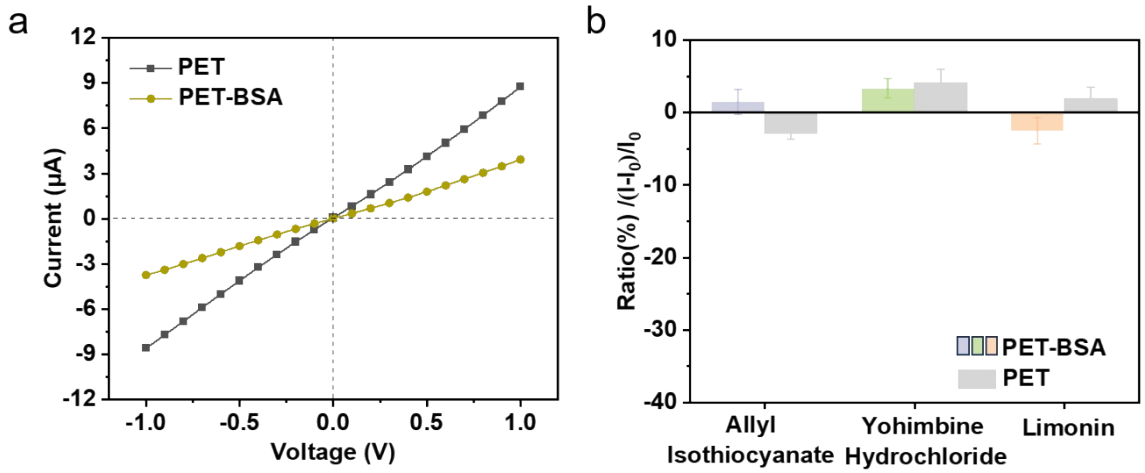

Figure S12. Characterizations of PET membranes modified with non-specific protein BSA (PET-BSA). (a) Current-voltage (*I-V*) curves of PET nanochannels after BSA modification (PET-BSA). (b) Comparative ionic current change ratios for PET and PET-BSA in response to 10^{-4} M solutions of allyl isothiocyanate (AI), yohimbine hydrochloride (YH), and limonin (L), respectively. Compared with the unmodified PET nanochannels, the PET-BSA exhibited an obvious decrease in current, which is attributed to the reduction in effective pore size induced by BSA modification, analogous to the effect observed with PET-TR. Nevertheless, owing to the absence of specific interactions between BSA and the bitter molecules, the current change ratios for 10^{-4} M solutions of AI, YH, and L remained minimal for PET-BSA, fluctuating within a narrow range of -5% to 5%. Furthermore, no significant difference in current response was observed between PET control and PET-BSA. These results indicate that the PET-BSA does not exhibit recognition of bitter substances, further confirming the necessity of the bitter taste receptor protein T2R38 for sensor functionality.

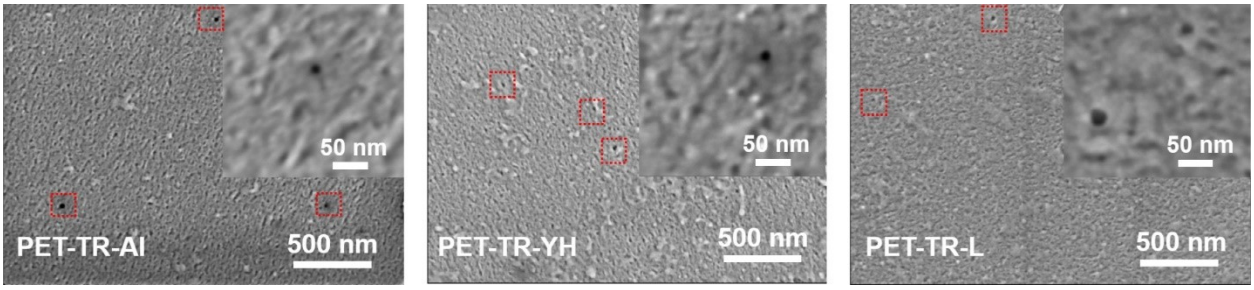

Figure S13. SEM images of the bitter receptors after binding to bitter substances.

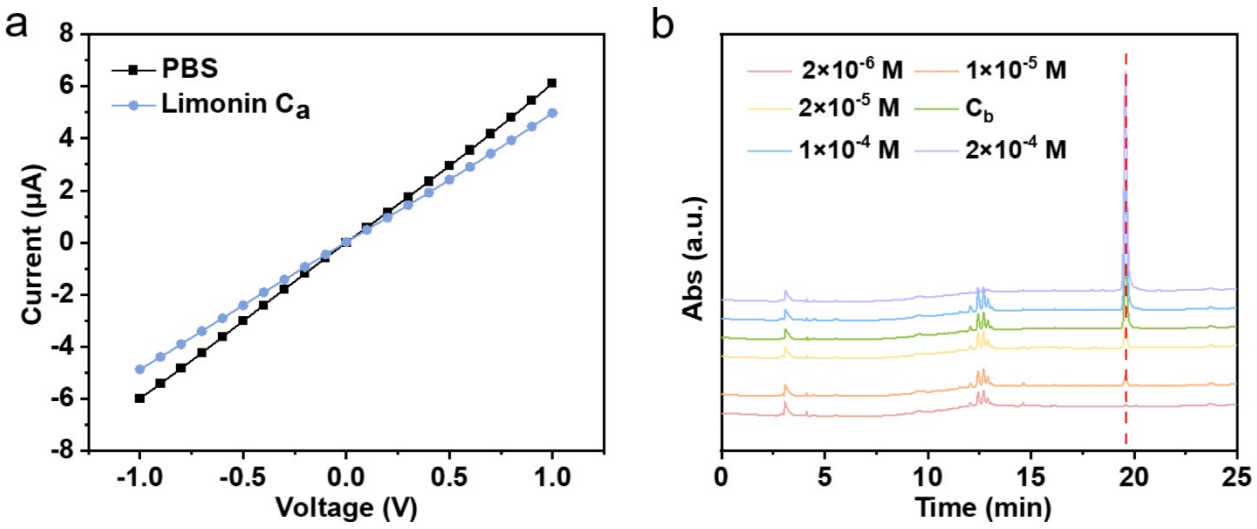

Figure S14. (a) *I-V* curves of limonin solution (C_0). (b) HPLC spectra of C_0 and five different concentrations of Limonin solutions.

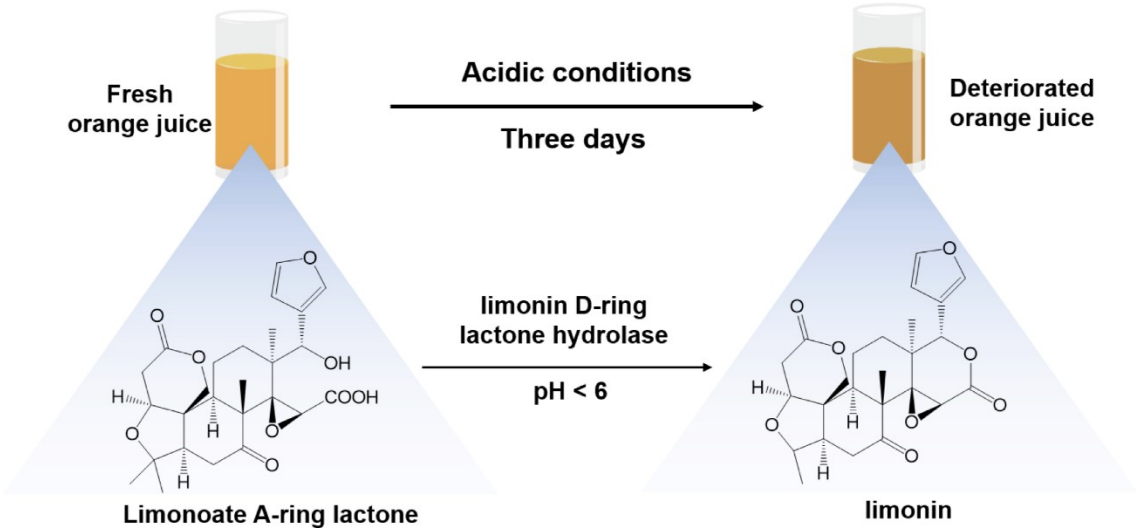

Figure S15. Limonin D-ring lactone hydrolase facilitates the conversion of limonoate A-ring lactone into bitter limonin.

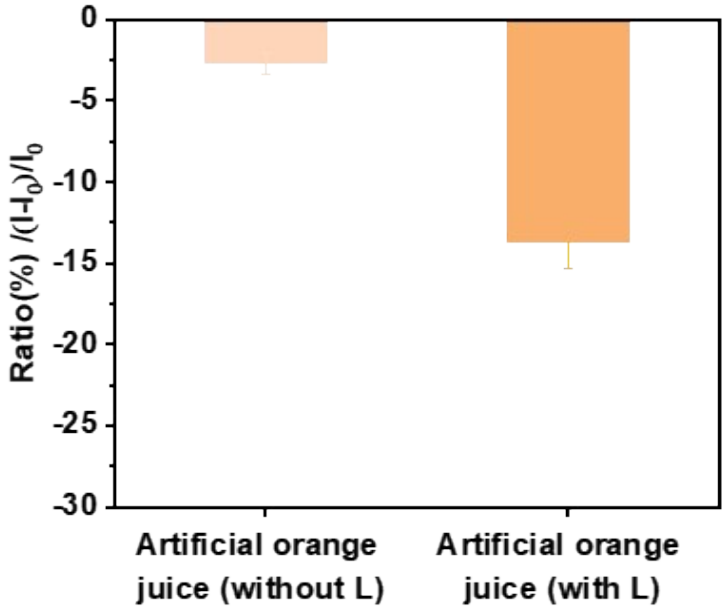

Figure S16. PET-TR bitter sensors for artificial orange juice samples with and without the addition of limonin (0.001%-0.002%), confirming that the other major components in orange juice do not interfere with the test.

Table S1. EDS mapping of the PET nanochannels membrane.

Element	Line	Apparent Concentration	k Ratio	Wt%
C	K series	202.77	2.02772	85.34
N	K series	4.47	0.00796	0.70
O	K series	75.81	0.25511	13.96
Total				100.00

Table S2. EDS mapping of the PET-TR nanochannels membrane.

Element	Line	Apparent Concentration	k Ratio	Wt%
C	K series	208.71	2.08710	86.66
N	K series	1.97	0.00351	0.42
O	K series	55.23	0.18585	12.89
S	K series	0.10	0.00088	0.03
Total				100.00

Table S3. The performance comparison of sensory evaluation, electronic tongues (ETs) and bioelectronic tongues (BioETs).

Techniques	Sensing elements	Bitter substance	LOD	Selectivity	Linear Range	Sample volume	Response time	Stability	Application scenarios	Ref
Sensory evaluation	Tongue	7-Ketologanin, Sweroside, Loganin	11.9 μg·mL^{-1}, 33.5 μg·mL^{-1}, 60.2 μg·mL^{-1}	High	N/A	18 mL	N/A	N/A	To identify the bitter compounds of blue honeysuckle	9
	Tongue	Caffeine, L-isoleucine, L-leucine, L-phenylalanine, L-tyrosine, L-valine	500 μM, 11000 μM, 12000 μM, 58000 μM, 5000 μM, 21000 μM	High	N/A	75 mL	N/A	N/A	To study the taste of black tea taste	10
	Tongue	Xanthotoxol, Oxypeucedanin hydrate, Isoimpinellin, Bergapten, Oxypeucedanin, imperatorin	0.1875 μg·mL^{-1}, 1.091 μg·mL^{-1}, 0.3263 μg·mL^{-1}, 3.905 μg·mL^{-1}, 17.43 μg·mL^{-1}, 81.35 μg·mL^{-1}	High	N/A	14 mL	10 s	N/A	To identify the bitter compounds of Hangbaizhi	11
ETs	The sensor array consisted of 16 prepared sensors with a polymer membrane	Rosuvastatin	N/A	Poor	2×10^{-5} - 2×10^{-3} M	50 mL	10 ~ 30 s	N/A	To evaluate the taste-masking efficiency of rosuvastatin sprinkle formulations	16
	TS-5000Z taste sensing system equipped with 4 sensor electrodes	Etofylline, Proxyphylline, Diprophylline	1.51 mM, 0.48 mM, 0.47 mM	Poor	3 - 100 mM	N/A	30 s	N/A	To detect xanthine derivatives in pharmaceuticals	17
	Four lipid membrane sensors of bitterness containing six taste factors	Andrographis herba	N/A	Poor	0.5 - 20 mg·mL^{-1}	100 mL	30 s	N/A	To measure the Bitterness of Andrographis Herba	18

Techniques	Sensing elements	Bitter substance	LOD	Selectivity	Linear Range	Sample volume	Response time	Stability	Application scenarios	Ref
BioETs	Quartz crystal microbalance device modified with bitter receptor	Denatonium	5 nM	High	10 nM - 0.1 mM	N/A	N/A	Stable for 7 days when stored at 4℃	To detect bitter substances	26
	Taste organoids coupled to a microelectrode array	Phenylthiourea (PTC)	1.56 mg mL^{-1}, 0.25 g mL^{-1}, 0.01 mmol L^{-1}, 3 mol L^{-1}	High	N/A	N/A	3 min	N/A	To distinguished sour, sweet, bitter, and salty stimuli	27
	Graphene field-effect transistor immobilized with bitter taste receptors nanodiscs	Salicin, saccharin	100 fM	High	10 pM ~ 100 pM; 100 pM ~ 1 nM	N/A	N/A	N/A	To detect the antagonism-based masking of bitterness	28
	Nanochannels modified with bitter taste receptor	Allyl Isothiocyanate (AI), Yohimbine Hydrochloride (YH), Limonin (L)	0.262 pM, 0.018 pM, 0.231 pM	High	10^{-4} -10^{-12} M, 10^{-4} -10^{-13} M, 10^{-4} -10^{-12} M	2 mL	2 min	Stable when stored at 4°C. Activity retained 91.81%, 90.24% and 83.15% of the initial performance for AI, YH and L after one week, respectively	To detect bitter substances	**This work**

Table S4. Energy of molecular docking of T2R38 with Allyl Isothiocyanate (AI), Yohimbine hydrochloride (YH), Limonin (L).

Ligands	Affinity (kcal/mol)
Allyl isothiocyanate (AI)	-3.2
Yohimbine hydrochloride (YH)	-7.9
Limonin (L)	-8.9